Journal of the European Ceramic Society 21 (2001) 19–27

www.elsevier.com/locate/jeurceramsoc

The manufacture of partially-stabilised and fully-stabilised zirconia fibres blow spun from an alkoxide derived aqueous sol–gel precursor

R.C. Pullar [1], M.D. Taylor, A.K. Bhattacharya *

Warwick Process Technology Group, School of Engineering, University of Warwick, Coventry CV4 7AL, UK

Received 8 March 2000; received in revised form 1 May 2000; accepted 4 June 2000

Abstract

Aligned fibres of partially stabilised zirconia (PSZ, 4 mol% Y_2O_3) and fully stabilised zirconia (FSZ, 8 mol% Y_2O_3), 3–5 μm in diameter, were blow spun from a sol–gel precursor, and then fired to give the ceramic fibre. Various potential sol precursors were investigated and characterised, the optimum being an aqueous sol made from hydrolysed and peptised zirconium iso-propoxide. The resulting zirconia fibres were characterised and their evolution studied by XRD, DTA/TGA and SEM, and their mechanical properties assessed. It was found that both PSZ and FSZ fibres formed poorly crystalline cubic zirconia at only 200°C, which became fully crystalline after firing to 400°C. The cubic form was the only phase seen in the FSZ fibre, whereas the PSZ fibre formed the tetragonal phase after firing between 1000 and 1200°C/3 h, and all fibres were nanocrystalline (grain diameter < 0.1 μm). Unusually the monoclinic form of zirconia was never observed in the PSZ fibres. After firing above 1200°C the fibres had a strain to break of 0.59%, and appeared to be well sintered from shrinkage data. They had superior creep resistance to *Saffil* zirconia fibres, creeping at temperatures 50°C higher.

Keywords: Creep; Fibres; Sol–gel methods; ZrO_2; ZrO_2 fibres

1. Introduction

Continuous zirconia fibres are of interest as high strength reinforcement materials, with a higher melting point of over 2700°C and better chemical resistance to reactive environments than alumina. Zirconia fibre could also be used for its dielectric properties, as an electrode in fuel cells and as a substrate for other oxides, and for these high performance applications the degree of control over microstructure achieved from the sol–gel process is required. The only commercially available zirconia fibres are *Zircar* fibres produced by Union Carbide from a rudimentary process, in which cellulosic fibres are impregnated with zirconium salts, and the organic matrix then burnt off.[1]

To produce a high strength zirconia fibre a small grain structure below 0.5 μm must be obtained by the addition of 1.5–5 mol% magnesia, calcia, ceria or yttria, so the crystal structure is partially stabilised in the tetragonal phase (PSZ) at room temperature.[2] With dopants below this level; a much larger grain size forms, giving the usually higher temperature monoclinic phase also at room temperature. When stressed the tetragonal material reverts back to the monoclinic phase, the transformation resulting in microcracking which weakens the fibre's tensile strength but allows it to absorb fracture energy.[3] The tetragonal phase is stable up to 1600°C but it is degraded by ageing in a moist environment at much lower temperatures,[4] so for use at very high temperature or in reactive environments the cubic phase may be more suitable. This can be achieved at room temperature by doping the zirconia with 8 mol% yttria, to form fully stabilised cubic zirconia (FSZ).

In 1987, a 2–5 μm diameter fine fibre was hand drawn from an acetate solution, and heated to 1000°C to give the tetragonal phase, which was maintained until it changed phase at 1600°C. This tetragonal phase resulted

* Corresponding author.

E-mail address: akb@warwick.ac.uk (A.K. Bhattacharya), r.c.pullar@sbu.ac.uk (R.C. Pullar).

[1] Now with the Centre for Physical Electronics and Materials, School of Electrical, Electronic and Information Engineering, South Bank University, 103 Borough Road, London SE1 0AA, UK.

0955-2219/01/$ - see front matter
PII: S0955-2219(00)00178-3

in a strength of up to 2.6 GPa in 3 μm fibres, higher than any alumina-based fibre.[5] Since then continuous stabilised zirconia fibres have been produced from the either the pyrolysis of an organic precursor fibre[6] or the extrusion of a precursor polymer,[7] but these processes typically result in a thicker fibre of around 20 μm which does not form the tetragonal phase until over 1100°C, resulting in a larger grain size and a lower tensile strength comparable to alumina fibres. In previous work, we have described the preparation of yttrium aluminium garnet fibres,[8] strontium and zirconium titanate fibres,[9,10] mullite fibres[11] and a range of magnetic ferrite fibres[12–16] in a demonstration programme to show how refractory and effect aligned fine fibres can be made by aqueous sol–gel routes. This present paper presents the preparation of nanocrystalline fibres of partially stabilised zirconia (PSZ) and fully stabilised zirconia (FSZ) from an aqueous sol–gel precursor.

2. Experimental

2.1. Preparative methods

2.1.1. Sol preparation

BDH analaR grade 2-propanol (IPA) was used, and dried with Rose Chemicals 3A molecular sieve when required, and all water used was distilled. The zirconia sols were made from Aldrich zirconium iso-propoxide, Zr(*i*-OPr)$_4$ (70% by weight in IPA). Several different permutations of sol preparation were investigated, all using Zr(*i*-OPr)$_4$ as the starting material:

2.1.1.1. Instant hydrolysis in excess water followed by peptisation. The Zr(*i*-OPr)$_4$ (0.1 mol = 32.76 g, 70% solution so needed 46.80 g of iso-propoxide solution) was instantly and fully hydrolysed by rapid addition to excess water with stirring, resulting in an instant thick off-white precipitate. This solid was ground up and dried at 105°C to produce 0.1 mol of Zr(*i*-OPr)$_4$ as a fine, dry powder. To this was added 0.1 mol of nitric acid (0.5 mol l^{-1}) resulting in instant bubbling and the of digestion of the hydroxide. This mixture peptised fully over one week to give a milky sol (0.13 mol l^{-1}).

2.1.1.2. Slow hydrolysis and simultaneous peptisation using excess water. 0.1 mol of the yellow Zr(*i*-OPr)$_4$was added to 200 ml of dry IPA to produce an off-white solution with no precipitation. A solution of nitric acid (0.5 mol l^{-1}) in a ratio of zirconia:acid of 1:1 was added dropwise to the propoxide solution with stirring. Immediately a thick gelatinous white precipitate formed, and more water was added when necessary to ease the mixing. A sol was formed in two hours (0.042 mol l^{-1}) and this was concentrated to 0.092 mol l^{-1} on a rotary evaporator.

2.1.1.3. Slow hydrolysis and simultaneous peptisation in stoichiometric amount of water. To a solution of Zr(*i*-OPr)$_4$ (0.1 mol) in 200 ml dry IPA was added a solution of 0.1 mol of concentrated nitric acid in 0.4 mol water. This was added dropwise with stirring and no precipitate was seen to form, until the solution turned cloudy after approximately half of the acidic solution had been added, but no thick precipitate formed. A cloudy sol (0.083 mol l^{-1}) had begun to form, but had not fully digested after 6 h. Upon standing over night a fine but gelatinous solid had settled out from the sol. This was concentrated to dryness on a rotary evaporator at a temperature of 35°C and a vacuum of 95 kPa leaving a sticky, yellow, glassy gel. This was redispersed in minutes with the addition of 50 ml water to give a clear sol (2.0 mol l^{-1}).

2.1.1.4. Slow hydrolysis and simultaneous peptisation in stoichiometric amount of water followed by immediate concentration and subsequent redispersal in water. A solution of 0.1 mol Zr(*i*-OPr)$_4$ in 200 ml dry IPA was made up, and a solution of 0.1 mol concentrated nitric acid and 0.4 mol water in 40 ml IPA was added dropwise with stirring. Immediately the solution turned cloudy, and again after approximately half the acidic solution had been added a thick white precipitate formed, and more IPA had to be added to allow mixing. Ten ml water was added to the cream coloured suspension (0.29 mol l^{-1}) and it was concentrated to dryness on a rotary evaporator at a temperature of 35°C and a vacuum of 95 kPa. This resulted in a sticky yellow solid (3.16 mol kg^{-1}), which redispersed in one hour upon dilution to 1.25 mol l^{-1} with water. Both the solid and redispersed sol still smelled strongly of alcohol, and they were again concentrated on the rotary evaporator to form dryer yellow crystals (4.69 mol kg^{-1}) with less odour of IPA. These were redispersed to a clear yellow sol of 1.88 mol l^{-1} in minutes. This sol was then left in a fume cupboard over a weekend and allowed to evaporate in air, leaving dry, bright yellow crystals with no residual odour of IPA, and this was redispersed in minutes to from a clear yellow sol (1.88 mol l^{-1}).

2.1.1.5. Slow hydrolysis and simultaneous peptisation in excess water followed by immediate concentration at 90°C and subsequent redispersal in water. Zr(*i*-OPr)$_4$ (0.1 mol) was diluted with 200 ml of dry IPA, and to this a solution of 1 mol water, 0.1 mol concentrated nitric acid and 50 ml IPA was added dropwise with stirring. A thick gelatinous precipitate formed, and this mixture was immediately concentrated on a rotary evaporator at a temperature of 35°C and a vacuum of 95 kPa. To prevent the sol from drying out, when it had been reduced to approximately 1 mol l^{-1} it was rediluted to 0.2 mol l^{-1} with water and reconcentrated. This was repeated twice to give a yellow sol with a concentration of 1.16 mol l^{-1}.

2.1.1.6. Preparation of the yttria sol. The yttria sol was produced via the peptisation of yttrium hydroxide as previously reported in the manufacture of yttrium aluminium garnet (YAG) fibres.[17] A yttrium salt solution 0.25 mol l^{-1}) was titrated to pH 9.5 with 4% ammonia solution at room temperature, and the gelatinous precipitate was filtered and washed with distilled water which had a pH of 5. The resulting firm but fondant-like cake, which was only 10% $Y(OH)_3$ by weight, was then peptised at room temperature with 0.5 M nitric acid in a ratio of yttrium:acid of 2:1. The precipitate began to digest immediately, and within an hour a sol had started to form. After stirring at room temperature for 12 h all of the solid had been peptised to form a slightly milky yttria sol of pH 7 (0.70 mol l^{-1}).

2.1.1.7. Preparation of mixed zirconia–yttria sols. Stoichiometric amounts of the yttria sol were added to a zirconia sol to form the required mixtures for PSZ (4 mol% Y_2O_3, $Zr_{0.92}Y_{0.08}O_{1.96}$) and FSZ (8 mol% Y_2O_3, $Zr_{0.84}Y_{0.16}O_{1.92}$) ceramic fibres.

2.1.2. Fibre preparation

The mixed zirconia–yttria sol was filtered through a 0.7 μm filter and then rendered spinnable by the addition of a small amount (2%) of polyethylene oxide (PEO) spinning aid and further concentration. The fibres were produced by a modified proprietary blow spinning process[18] in which the spinning solution was extruded through a row of holes, on either side of which impinge parallel jets of humidified attenuating air. The fibres were gelled by mixing in a stream of hot secondary air and then collected both in a basket as a random staple and on a rotating drum as an aligned blanket. A notable feature of the gel and spinning process was that the fibres were generated at 9 m s^{-1} and set within 1 s. After collection the fibres were removed and stored in a circulating oven at 110°C to await subsequent heat treatment.

2.1.3. Heat treatments of fibres

The gel fibres were fired at 100°C/h to 400°C and kept at this temperature for two hours to remove any organic or nitrate components, and then further heated at 300°C/h to the desired temperature, where they were maintained for 3 h unless otherwise stated.

2.2. Characterisation

2.2.1. Photon correlation spectroscopy (PCS)

The particle sizes of the sols were measured on a Malvern Instruments Lo-C Autosizer and series 7032 multi-8 correlator, using a 4 mw diode laser, 670 nm wavelength. The scattered light was detected at a fixed angle of 90° to the incident laser beam. This has been certified by the manufacturers to measure inorganic sol species of 3 nm diameter and above, provided the difference between the refractive indexes of the solvent and particle are sufficiently large. This was the case with our samples, the refractive indexes used being 1.33 for the solvent (water), 1.73 for the yttria sol and 1.70 for the zirconia and mixed sols. This piece of equipment conforms to the Methods of particle size determination standards, ISO 13321, part 8 — PCS (1996) and BS3406, part 8 — PCS (1997) for determination of the Z average calculated from the monomodal cumulants analysis. The volume and number distribution particle sizes and ranges were calculated from the cumulants results using the Malvern PCS software version 1.32 in multimodal mode. The volume distribution is a measure of the volume occupied by particles against their size, and the number distribution is a simple assessment of the particle size distribution, and these two values most accurately reflect the true nature of the sol.

Five drops of the sol were added to a cuvette of distilled water, after both had been filtered through a 0.8 μm filter. This dilution had no apparent effect upon the stability of the sol, and there was no change in size distribution of the PCS sample after standing for 24 h. The sols were measured in 30 runs over 20 min, and the average values calculated from this, and this was repeated three times to ensure reproducibility.

2.2.2. X-ray powder diffraction (XRD) measurement

X-ray powder diffraction patterns of the samples treated at various temperatures were recorded in the region of $2\theta = 10-80°$ with a scanning speed of 0.25°/min on a Philips PW1710 diffractometer using CuK_α radiation with a nickel filter. Philips APD 1700 software was used to calculate the average size of the crystallites in a sample using the Scherrer equation:

$$D = K\lambda/h_{1/2}\cos\theta$$

where D = average size of the crystallites, K = Scherrer constant (0.9×57.3), λ = wavelength of radiation (1.5405 Å), $h_{1/2}$ = peak width at half height and θ corresponds to the peak position.

2.2.3. Scanning electron microscopy (SEM)

Scanning electron micrographs and analysis of the morphology of the samples was carried out on a Cambridge Instruments Stereoscan 90 SEM operating at 5 kV. Conducting samples were prepared by gold sputtering fibre specimens.

2.2.4. Porosity and sintering estimates

The weight loss and shrinkage in length of the fibres was measured over a range of temperatures from 110 to 1400°C. The ultimate shrinkage from sol to gel, and then to fully dense refractory can be calculated from the concentration of ceramic at different stages of the pro-

cess and reasonably accurate estimates of sol and gel densities. The porosity of fibres during a firing sequence can then be inferred from the linear shrinkage of an aligned sample of fibre, assuming that the fibre is fully sintered when no more shrinkage occurs. To calculate the estimated porosity it was assumed that the shrinkage occurred uniformly in all three dimensions of the individual fibres. The estimated porosity was then calculated from the equation:

$$P = 1 - \left(\frac{1 - S}{1 - S_T}\right)^3$$

where S_T = % linear shrinkage measured at a given temperature, S = total% linear shrinkage for fully sintered material and P = % calculated porosity. This method provides only an estimate, with the error becoming greater as porosity increases, and is unreliable for values of $S < 0.5S_T$.

2.2.5. Differential thermal analysis (DTA) and thermogravimetric analysis (TGA)

Simultaneous differential thermal analysis and thermogravimetric analysis (DTA–TGA) was performed on gel fibres in flowing air up to a temperature of 1000°C at a rate of 10°C min^{-1}, using a Rheometric Scientific STA 1500. Due to the rapidity of this heating rate, features may occur at a temperature slightly higher than normal for the same event under a slower heating regime.

2.2.6. Estimation of strain-to-break

Strain-to-break was estimated using the wire indentation stress test, which was done by gluing a thin strip of fibres on to the surface of transparent double sided adhesive tape which in turn was glued to a soft rubber pad. The blanket was indented with stainless steel wires of reducing diameter from 1.2 down to 0.3 mm, and the wires were held in toolmaker's clamps and pressed into the sample. The tape was then carefully removed with the adhering fibre strip from the rubber pad, and the lines of indentation examined for lines of breakage under an optical microscope at 100× magnification.

2.2.7. Creep measurements using the bend stress relaxation (BSR) technique

High temperature creep behaviour may be sensitive to small changes in formulation and may also be optimised the early stages of a development. The Bend Stress Relaxation (BSR) technique was developed by Morscher[19] and has been used in previous work to rank the creep performance of polycrystalline YAG fibres.[17] The test was carried out on strips of aligned YAG fibre 1×10 mm, with the longer dimension parallel to the axis of alignment. These fibres were prefired to a nearly or fully sintered state, so any observed effect was due to creep, and not a sintering effect.

In the test, the fibre was sandwiched between a 5.6 mm alumina rod resting on two other larger rods of 8.0 mm diameter (Fig. 1). The fibre was therefore bent to a known initial diameter, d_0 (= 5.6 mm), imposing a surface strain given by d/d_0 where d = the fibre diameter. The fibre was then heated to various temperatures where it was held for 1 h, and then allowed to cool down immediately in air to room temperature and the strain-inducing rod removed. If a stress relaxation has taken place and creep has occurred the fibre retains a residual curvature of diameter d_f. The stress relaxation ratio, M, can then be calculated from the equation:

$$M = 1 - \frac{d_0}{d_f}$$

If $M = 1$, this means that no creep has taken place, while $M = 0$ indicates that the fibre has undergone total stress relaxation and crept around the diameter of the rod. These results can then be plotted against temperature and compared to previous results. The rod size was chosen so that even the smallest fibres (3 μm diameter) were subjected to less than 0.15% strain, and the diameter of creep could be measured with a reasonable degree of accuracy (±0.4 mm). Morscher indicated that during the BSR test a sample undergoes a creep strain proportional to (1/M)-1 so that the technique may be used to make approximate quantitative comparisons.

3. Results and discussion

3.1. Sol formation and characterisation

In all the sols, the size of the sol particles were found to be sensitive to the preparative techniques and conditions employed, and PCS enabled us to measure and control the properties of the sol. The volume distribution of the sol particles has a direct effect on the spinning process, and even a small number of large particles can severely impede or even nullify the spinnability of the sol. Therefore volume distribution, especially the upper limit, was considered a more relevant measure than the Z average. The sols are discussed in the same order and identified as in Experimental.

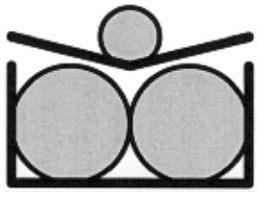

Fig. 1. Cross-sectional diagram of the fibre–alumina rod sandwich in BSR test.

i. The first method of zirconia sol formation attempted was by the complete hydrolysis of zirconium iso-propoxide followed by subsequent digestion in acid. This direct hydrolysis of the iso-propoxide resulted in a sol with a volume average of 152 nm and a range between 70 and 400 nm (Fig. 2i). This is known from experience to be much to large to be successfully spinnable by our technique, for which a volume average of below 50 nm and an upper limit of no more than 100 nm is preferable. Therefore, the remaining experiments focused on simultaneous hydrolysis and peptisation of the alkoxide.

ii. The addition of excess water directly to the iso-propoxide appeared to hydrolyse it too rapidly and probably incompletely, as it resulted the in the precipitation of coarse particles which did not breakdown much in the digestion process. Although a sol seemed to have formed within 2 h, the PCS measurement was not taken until the following day to allow further peptisation to occur. Despite this the sol consisted of particle even larger than in (i), with a volume average of 216 nm and a wide range of 120–600 nm, as shown in Fig. 2ii.

iii. Considering the results above, it was decided to limit the amount of water by using a stoichiometric amount (4:1 to zirconia) and concentrated acid during the hydrolysis of the iso-propoxide. The thick precipitate did not from on addition, but the cloudy sol which resulted had a very large volume distribution from 130 to 800 nm, and this reached up to 2 μm if the sol was not filtered. Indeed, the cloudy mixture was not a true sol, as evidenced by the separation on standing. After redispersion however the sol characteristics were greatly improved, it having formed a stable sol with a volume average of 99 nm and a small range of 80–130 nm (Fig. 2iii).

iv. Following the results above, it was decided to concentrate the solution immediately after addition of water and acid, and in an attempt to prevent the separation of the sol. After concentration on the rotary evaporator and redispersal the yellow sol still consisted of large particles with a volume average of 233 nm and a range between 140 and 450 nm, and further evaporation on this apparatus gave no improvement. The sol still contained IPA, as evident from its odour, and so it was left to evaporate in air at room temperature in a fume cupboard over a weekend. This removed all the smell of IPA, and the redispersed sol demonstrated an improved volume average of 169 nm, and although the upper limit was 300 nm, 98% of the volume distribution formed a narrow peak at 140–200 nm (Fig. 2iv).

v. As long as the water was added slowly in a solution of IPA along with the acid, the immediate evaporation and removal of all IPA appeared to be the major size determining process of the sol, rather than the actual hydrolysis of the iso-propoxide. Therefore an excess of water was used in the hydrolysis step and water was added at regular stages during the concentration of the suspension, so that the sol was never totally dried out but the IPA was removed as an azeotropic mixture. To aid this process the solution was concentrated on a rotary evaporator at 90°C and under a vacuum of 95 kPa. The sol thus produced had the smallest volume distribution of all with a volume average of 33 nm. The range was 20–80 nm, and 95% of the particles were in a sharp peak between 20 and 50 nm (Fig. 2v), making this zirconia sol suitable for use in the blow spinning process. This sol was stable for several months.

vi. The yttria sol continued to peptise upon standing to give a volume average of 44.3 nm and range of 20–200 nm (Fig. 3vi) after standing at room temperature for 1 week. After this period no further improvement was observed, and the sol remained stable for over 2 months.

vii. The zirconia and yttria sols produced from (v) and (vi) mixed well and remained stable when added to each other in the two stoichiometric ratios to yield the PSZ (4 mol% Y_2O_3, $Zr_{0.92}Y_{0.08}O_{1.96}$) and FSZ (8 mol% Y_2O_3, $Zr_{0.84}Y_{0.16}O_{1.92}$) ceramic products. The PCS plot of the mixed sols lay between those of the two constituent sols, closer to the major zirconia sol component. The volume distribution of the FSZ precursor sol is compared to the component sols in Fig. 3, having a volume average of 39 nm and a range of 25–95 nm, with 92.5% of the sol particles being between 25 and 50 nm.

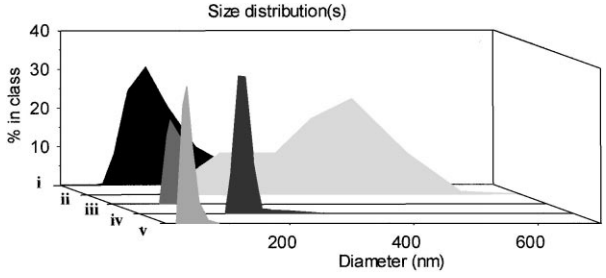

Fig. 2. Comparison of particle volume distributions of the zirconia sols prepared by methods (i)–(v), as detailed in Section 2.1.1.

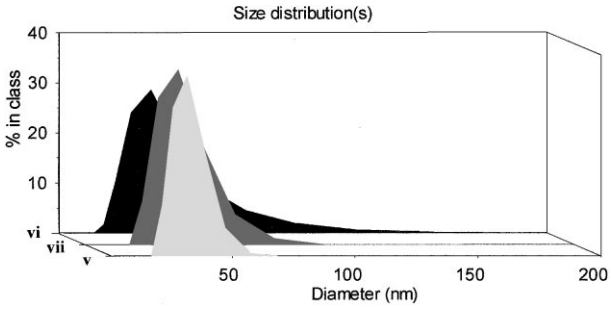

Fig. 3. Comparison of particle volume distributions of zirconia sol prepared by method (v) in section 2.1.1, yttria sol (vi) and mixed sol (vii), of stoichiometric composition $Zr_{0.84}Y_{0.16}O_{1.92}$.

3.2. Crystallisation, evolution and microstructrure of PSZ and FSZ fibres

Gel fibres were spun from sol (vii) with the stoichiometric compositions for PSZ and FSZ. The continuous fibres were 4–5 μm in diameter, had smooth, even sides, and aligned fibres retained their alignment after firing up to 1400°C. The XRD pattern of the FSZ fibres over a range of temperatures is shown in Fig. 4, and it can be seen that after firing at only 200°C cubic zirconia had begun to crystallise from the amorphous background. By 400°C, this had fully crystallised with a crystallite size of 17 nm, it was 19 nm at 600°C and by 1200°C this had grown to only 28 nm. Likewise, the PSZ fibres formed the cubic phase at low temperatures, but did not form a pure tetragonal phase stable at room temperature until fired to between 1000 and 1200°C/3 h (Fig. 5). This agrees with previously reported fibres made organic precursors,[6,7] although at only 600°C the single peaks of the cubic pattern are showing signs of widening and shoulders as the tetragonal phase is beginning to form (Fig. 5). The crystallite size of the tetragonal phase was larger than that of cubic at equivalent temperatures, being 22 nm at 600°C and 53 nm at 1200°C. Unusually, the monoclinic phase was never seen, as this is the natural crystalline phase for unstabilised zirconia up to 1000°C, and either monoclinic or a mixture of cubic and monoclinic is the normal precursor phase to the tetragonal phase in PSZ.[20] None of the zirconia fibres had any grains or pores discernible from SEM, and therefore the grains were all below 0.1 μm, with the FSZ fibre fired to 1200°C/3 h shown in Fig. 6 being typical.

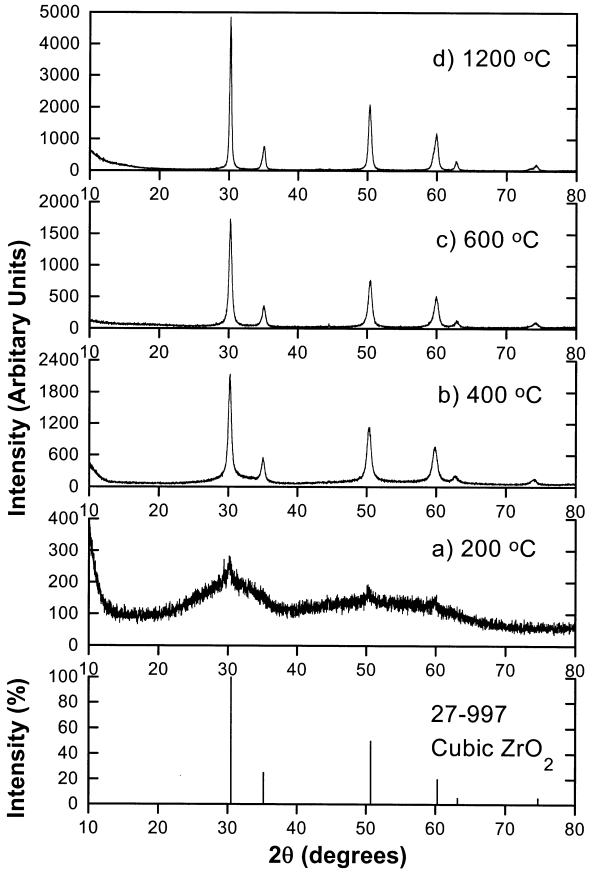

Fig. 4. XRD pattern of FSZ fibres heated at (a) 200, (b) 400 (c) 600 and (d) 1200°C for 3 h.

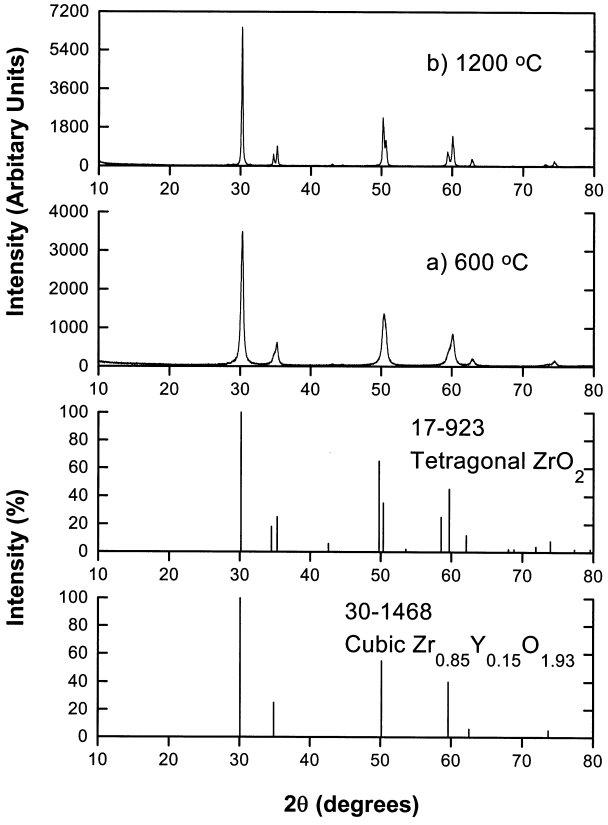

Fig. 5. XRD pattern of PSZ fibres heated at (a) 600 and (b) 1200°C for 3 h.

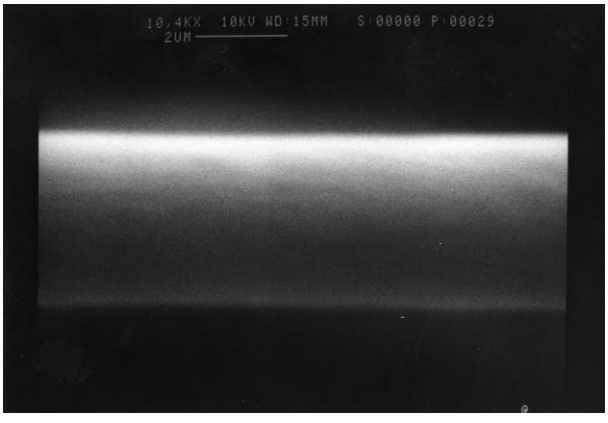

Fig. 6. SEM micrograph of FSZ fibres fired at 1200°C for 3 h.

Table 1
Comparison of the weight loss, linear shrinkage and estimated porosity of PSZ ($Zr_{0.92}Y_{0.08}O_{1.96}$) and FSZ ($Zr_{0.84}Y_{0.16}O_{1.92}$) fibres (n/a = results not available)

	PSZ ($Zr_{0.92}Y_{0.08}O_{1.96}$) fibre			FSZ ($Zr_{0.84}Y_{0.16}O_{1.92}$) fibre		
Temperature (°C)	Weight (%)	Shrinkage (%)	Porosity (%)	Weight (%)	Shrinkage (%)	Porosity (%)
400	n/a	n/a	n/a	35.60	20.83	39.0
600	49.08	29.29	19.5	41.90	28.57	17.0
800	49.76	30.00	17.3	42.53	29.63	13.1
1000	50.25	32.14	9.2	43.43	30.00	11.8
1200	50.56	33.57	3.2	43.97	31.34	6.5
1400	51.67	34.29	0	44.16	32.86	0

The weight loss and shrinkage data for both zirconia fibres are shown in Table 1, along with the estimated porosity calculated from linear shrinkage results, and most shrinkage and weight loss had occurred by 600°C. This can also been seen from the DTA/TGA plots for FSZ fibres in Fig. 7, which show a total weight loss of 40% at 1000°C. There was a slight endotherm around 90°C corresponding to water loss, and around 15% weight was lost from this drying process. There was a sharp exotherm at 220°C with a simultaneous sudden weight loss of 5%, caused by the combustion of volatile organic compounds, which caused a small heat excursion exceeding the heating rate. The second less extreme exotherm at 280°C is observed in all fibres blow spun from this process, and is due to the polymeric spinning aid being lost. The 10% weight lost between 220 and 550°C must be due to the loss of nitrates, as well as any residual water locked up in small pores, but it was a much more gradual process than the runaway exotherms observed in our YAG fibres reported previously.[17] This could be moderated by the gradual crystallisation of the cubic zirconia phase between 100 and 400°C, as suggested by the XRD patterns, whereas the YAG fibres remained amorphous until over 700°C. The last sudden weight loss of 5% between 500 and 550°C was not observed in previous fibres produced at Warwick, all of which were spun from sols peptised from inorganic hydroxides and doped with metal salts. Therefore, it could be a feature of the alkoxide derived zirconia sol, perhaps due to the loss of alcohols trapped in very small pores, and corresponded to a shrinkage of 8% between 400 and 600°C.

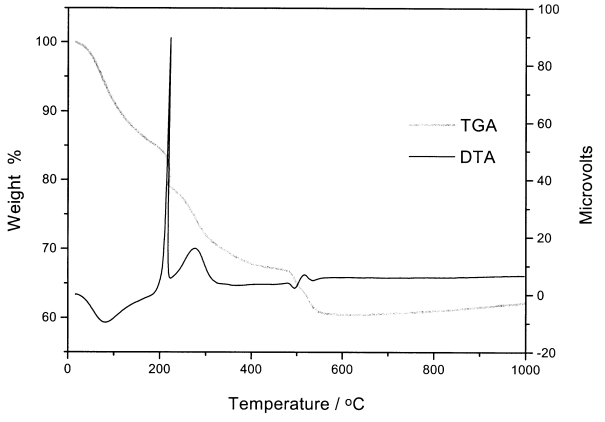

Fig. 7. DTA/TGA plots for FSZ fibres heated to 1000°C at 10°C min^{-1}.

Shrinkage data indicated that at 400°C the fibres were still very porous, and in both cases the fibres were still quite poorly sintered at temperatures over 1000°C (Table 1). Although the PSZ fibre had undergone more shrinkage and weight loss than the FSZ fibre at 600°C, at which point the majority of these processes had occurred, and was estimated to be more porous as well, at higher temperatures over 1000°C it appeared to be better sintered than the FSZ fibre. The differences in weight loss and shrinkage could be due to differences in concentration of the sols prior to spinning, an unavoidable feature in this small scale development process, and the superior degree of sintering seems to occur with the onset of the tetragonal phase. It must be noted that the porosities detailed here were only crude estimates from shrinkage data, assuming that as there was no further shrinkage above 1400°C, the fibre was fully sintered at this temperature. However, it is quite possible that some porosity remains at this temperature, and that these porosity values are underestimates. After firing to 1200°C, the fibre had an average diameter of 3.7 μm, and the FSZ fibre had a strain to break of 0.46 and 0.59% when fired to 1200 and 1300°C, respectively. This compares well to 0.48% measured for 3 μm *Saffil* zirconia fibres,[21] and YAG and BaM ferrite fibres made by the same sol–gel process had strain to break of 0.64% at 1400°C[17] and 0.67% at 1000°C[14], respectively. As both low porosity and grain size are required for a strong fibre,[22] this was a good indication that the zirconia fibres were well sintered at 1400°C, and that the porosity estimates were reasonably accurate.

The creep of PSZ and FSZ fibres prefired to 1200°C was assessed using the BSR test, and compared to *Saffil* zirconia fibre also prefired to 1200°C, which has been assessed by the same method previously.[21] It can be seen

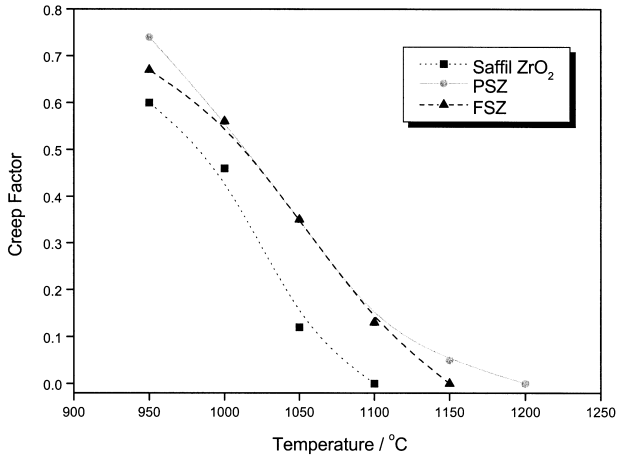

Fig. 8. Comparison of the creep of PSZ and FSZ fibres and *Saffil* zirconia fibres, all prefired to 1200°C/3 h.

from Fig. 8 that both zirconia fibres reported here out performed the *Saffil* zirconia fibre, creeping at approximately 50°C higher, and with a creep rate estimated to be 4 times slower at 1050°C. It can also be seen that the PSZ fibre had slightly superior creep resistance than FSZ at temperatures over 1100°C, although both had fully crept by 1200°C. As with YAG fibres,[17] once creep commences all of the fibres have crept fully with a temperature rise of around 200°C.

4. Conclusions

Gel precursor fibres for PSZ and FSZ were successfully spun from combined zirconia and yttria sols. The zirconia sol was made from a peptised solution of zirconium iso-propoxide in IPA, hydrolysed with an excess of water followed by the removal of the IPA. This gave a spinnable zirconia sol with 95% of the particles between 20 and 50 nm in diameter, making this zirconia sol suitable for use in the blow spinning process. When added to the yttria sol, made from peptised yttrium hydroxide and with a larger particle size of 44 nm, the resulting mixed sol had an average particle diameter of 39 nm, between those of the two constituent sols, and closer to the major zirconia sol component.

The ceramic fibres retained their alignment upon heating, and had diameters between 3 and 5 μm. Both fibres had formed poorly crystalline cubic zirconia by 200°C, and this remained the sole phase of the FSZ fibres up to 1200°C, at which point they had a crystallite size of only 28 nm. The PSZ fibre formed the tetragonal phase when fired to between 1000°C and 1200°C/3 h, but with a larger crystallite size of 53 nm. The monoclinic phase was never observed. The PSZ fibre appeared to be more fully sintered at higher temperatures than the FSZ fibre, but both remained slightly porous to at least 1200°C. However, both had nanocrystalline microstructures, with no pores or grains observed in SEM micrographs, indicating a grain size below 0.1 μm. The strain to break of the FSZ fibre was measured as 0.59% when fired to 1300°C, comparable to commercially available fibres, and this was also an indication that the fibres were small grained and reasonably well sintered at this temperature. They had superior creep resistance to *Saffil* zirconia fibres, creeping at temperatures 50°C higher.

References

1. Naumann, A. W. and Gortsena, F. P. (Union Carbide Corp.), *Ger. Offen*. **2007209**, September 1970.
2. Garvie, R. C., Stabilization of the tetragonal structure in zirconia microcrystals. *Journal of Physical Chemistry*, 1978, **82**, 218.
3. Garvie, R. C., Hannink, R. H. and Pascoe, R. T., *Nature*, 1975, **258**, 703.
4. Tsubakino, H., Hamamoto, R. and Nozato, R., Tetragonal-to-monoclinic phase-transformation during thermal cycling and isothermal aging in yttria partially-stabilized zirconia. *Journal of Materials Science*, 1991, **26**, 5521.
5. Marshal, D. B., Lange, F. L. and Morgan, P. D., High-strength zirconia fibres. *Journal of the American Ceramics Society*, 1987, **70**, C-187.
6. Yogo, T., Synthesis of polycrystalline zirconia with organozirconium precursor. *Journal of Materials Science*, 1990, **25**, 2394.
7. Abe, Y., Kudo, T., Tomioka, H., Gunji, T., Nagao, Y. and Misono, T., Preparation of continuous zirconia fibres from polyzirconoxane synthesized by the facile one-pot reaction. *Journal of Materials Science*, 1998, **33**, 1863.
8. Pullar, R. C., Taylor, M. D. and Bhattacharya, A. K., The manufacture of yttrium aluminium garnet (YAG) fibres by blow spinning from a sol–gel precursor. *Journal of the European Ceramic Society*, 1998, **18**, 1759.
9. Pullar, R. C., Taylor, M. D. and Bhattacharya, A. K., Blow spun strontium zirconate fibres produced from a sol–gel precursor. *Journal of Materials Science*, 1998, **33**, 3229.
10. Bhattacharya, A. K., Hartridge, A., Mallick, K. K. and Taylor, M. D., Inorganic sol gel synthesis of zirconium titanate fibres. *Journal of Materials Science*, 1996, **31**, 5583.
11. Bhattacharya, A. K., Hartridge, A., Mallick, K. K. and Taylor, M. D., A novel aqueous route for the synthesis of mullite fibres. *Journal of Materials Science Letters*, 1996, **15**, 1654.
12. Pullar, R. C., Taylor, M. D. and Bhattacharya, A. K., Novel aqueous sol–gel preparation and characterization of barium M ferrite, $BaFe_{12}O_{19}$ fibres. *Journal of Materials Science*, 1997, **32**, 349.
13. Pullar, R. C., Taylor, M. D. and Bhattacharya, A. K., Aligned hexagonal ferrite fibres of Co_2W, $BaCo_2Fe_{16}O_{27}$ produced from an aqueous sol–gel process. *Journal of Materials Science*, 1997, **32**, 873.
14. Pullar, R. C., Appleton, S. G. and Bhattacharya, A. K., The manufacture, characterisation and microwave properties of aligned M ferrite fibres. *Journal of Magnetism and Magnetic Materials*, 1998, **186**, 326.
15. Pullar, R. C., Appleton, S. G., Stacey, M. H., Taylor, M. D. and Bhattacharya, A. K., The synthesis and characterisation of aligned fibres of the ferroxplana ferrites Co_2Z, 0.67% CaO-doped Co_2Z, Co_2Y and Co_2W. *Journal of Magnetism and Magnetic Materials*, 1998, **186**, 313.
16. Pullar, R. C., Pyke, D. R., Taylor, M. D. and Bhattacharya, A. K., The manufacture and characterisation of single phase magnetite and haematite aligned fibres from an aqueous sol–gel process. *Journal of Materials Science*, 1998, **33**, 5229.

17. Pullar, R. C., Taylor, M. D. and Bhattacharya, A. K., The sintering behaviour, mechanical properties and creep resistance of aligned polycrystalline yttrium aluminium garnet (YAG) fibres, produced from an aqueous sol–gel precursor. *Journal of the European Ceramic Society*, 1999, **19**, 1747.
18. Morton, M. J., Birchall, J. D. and Cassidy, J. E., *UK Pat*. **1360197**, July 1974
19. Morscher, G. N. and Dicarlo, J. A., A simple test for thermomechanical evaluation of ceramic fibers. *Journal of the American Ceramic Society*, 1992, **75**, 136–140.
20. Duwez, P. S., Brown, F. H. and Odell, F., *Phase Diagrams for Ceramists*. American Ceramic Society, Columbus, OH 1964, Diag. **355**, p. 140 (from Journal of the Electrochemical Society **98**, 1951, 360).
21. Taylor, M. D. and Bhattacharya, A. K., The comparison of alumina and zirconia fibres using simple thermal and mechanical techniques. *Journal of Materials Science*, 1999, **34**, 1277.
22. Fulrath, R. M. and Pask, J. A. (eds.), *Ceramic Microstructures*. John Wiley and Sons Inc., New York, 1968.